Near-field microwave magnetic nanoscopy of superconducting radio frequency cavity materials

Tamin Tai,[1,2,a)] Behnood G. Ghamsari,[2] Thomas R. Bieler,[3] Teng Tan,[4] X. X. Xi,[4] and Steven M. Anlage[1,2,b)]
[1]*Department of Electrical Engineering, University of Maryland, College Park, Maryland 20742-3285, USA*
[2]*Department of Physics, Center for Nanophysics and Advanced Materials, University of Maryland, College Park, Maryland 20742-4111, USA*
[3]*Chemical Engineering and Materials Science, Michigan State University, East Lansing, Michigan 48824, USA*
[4]*Physics Department, Temple University, Philadelphia, Pennsylvania 19122, USA*

(Received 6 December 2013; accepted 26 May 2014; published online 10 June 2014)

A localized measurement of the RF critical field on superconducting radio frequency (SRF) cavity materials is a key step to identify specific defects that produce quenches of SRF cavities. Two measurements are performed to demonstrate these capabilities with a near-field scanning probe microwave microscope. The first is a third harmonic nonlinear measurement on a high Residual-Resistance-Ratio bulk Nb sample showing strong localized nonlinear response, with surface RF magnetic field $B_{surface} \sim 10^2$ mT. The second is a raster scanned harmonic response image on a MgB_2 thin film demonstrating a uniform nonlinear response over large areas. © *2014 AIP Publishing LLC*. [http://dx.doi.org/10.1063/1.4881880]

Materials issues limit the ability to mass-produce bulk Nb Superconducting Radio Frequency (SRF) cavities with consistent high accelerating gradient performance. Much debate regarding this inconsistent performance has concluded that certain types of defects on the Nb cavity surface behave as a source of quenching in high RF magnetic fields.[1,2] Quench occurs when the superconductor returns to the normal state in the presence of strong fields, thus limiting the utility of the entire SRF cavity. In addition, it is widely observed that the quality factor (Q) of SRF cavities falls dramatically with increasing surface RF magnetic field, particularly as the quench field is approached.[3] A detailed microscopic understanding of this Q drop is lacking but is most likely related to the inevitable defects on the inner surface of bulk Nb cavities.[1,2,4] These defects may be either non-superconducting or have lower critical temperature (T_c), making them sources of dissipation which interrupt the superconducting current flow.[5]

Unfortunately, it is difficult to totally remove all of these defects even after sophisticated physical and chemical treatments. Because different defects each have their own quench limit, not all of the defects behave as sources of quenching under given cavity operation conditions. Therefore, it is necessary to quantitatively understand the relation between physical defects and their individual electromagnetic properties such as local critical field. Currently, in order to isolate specific defects in SRF cavities, most measurements utilize a complete accelerator cavity[6] and image the quenching hot spots at high accelerating gradient via a thermometer array attached to the outside wall of the cavity.[2] Such measurements reveal the locations of quench sites only to within a few millimeters, far larger than the defect itself, making their unique identification difficult.

Microscopic techniques have not been used in the past because traditionally it is difficult to create strong and localized RF magnetic fields at the cavity operating frequency (several GHz).[7,8] Our idea is to look at the active surface of SRF cavities with a very intense and localized magnetic field (on the order of the thermodynamic critical field of bulk Nb) and directly measure the local electromagnetic response in the cavity operating regime at low temperature.[9,10] Our method is to integrate a magnetic write head from a longitudinal recording hard drive[11] into a near-field microwave microscope[12,13] and directly measure the local nonlinear response in the multi-GHz frequency regime at cryogenic temperatures. The microscope can study bulk samples from Nb cavities or any material of interest to the SRF community such as MgB_2 thin films.[14,15] Defective regions, which create quenches in SRF cavities, are expected to be strong sources of nonlinear response. Up to this point, localized nonlinear microwave response has only been measured from superconducting thin films.[12,13,16–21] Here, we measure a strong localized nonlinear response from the technologically relevant bulk Nb material.

In our first experiment, we measure the third harmonic scalar power (P_{3f}^{sample}) that is generated by the bulk Nb sample due to local harmonic excitation at a fixed location. The third-harmonic power is studied because it is sensitive to the extrinsic properties (i.e., associated with defects), almost always at a level far stronger than the intrinsic response[22] and background levels. Fig. 1 shows the schematic microwave circuit for sensing small P_{3f}^{sample} signals[13,16,17] from a bulk Nb superconductor. A schematic diagram of the sample is also shown. Both the magnetic probe and superconductor are kept in a high vacuum cryogenic environment. The magnetic write head is made by Seagate (Part No. GT5) and has a 100 nm wide magnetic gap. The microwave source generates an excitation wave (a fundamental tone) at frequency f which is sent into the magnetic write head probe through a

a)Email: tamin@umd.edu
b)Email: anlage@umd.edu

 © 2014 AIP Publishing LLC

This article is copyrighted as indicated in the article. Reuse of AIP content is subject to the terms at: http://scitation.aip.org/termsconditions. Downloaded to IP: 129.2.40.52 On: Fri, 19 Sep 2014 14:46:55

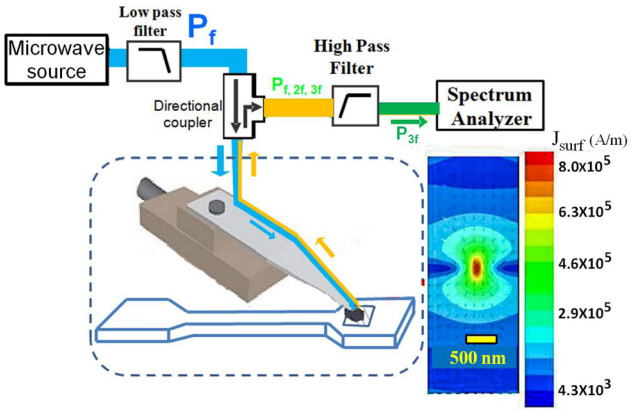

FIG. 1. Set up of the P_{3f} measurement in nonlinear microwave microscopy.[12,15,16] A fundamental tone is generated by the microwave source and is sent to the magnetic write head probe assembly on top of superconducting sample through the directional coupler. Then the reflected harmonic responses from the superconducting sample are shunted by the directional coupler and the selected harmonic response (P_{3f}) is analyzed by the spectrum analyzer. A schematic diagram of the high RRR bulk Nb sample is shown. The marked rectangle is the region where many single-fixed-point P_{3f} measurements are performed. A simulated surface current density distribution (J_{surf}) on the sample surface created by the magnetic write head probe is shown in the inset assuming that the probe height is 200 nm away from the sample surface.[13]

low pass filter (to eliminate harmonics) and directional coupler. The magnetic write head probe creates a localized and intense RF magnetic field on the surface of the bulk Nb sample (inset of Fig. 1), similar in spirit to the previous studies of magnetic materials.[23,24] The sample responds by creating screening currents to maintain the Meissner state in the material. These currents inevitably produce a time-dependent variation in the local value of the superfluid density, and this in turn will generate a response at harmonics of the driving tone.[17,25] The generated harmonic signals are gathered by the magnetic probe and returned to room temperature where they are high-pass filtered to remove the fundamental tone P_f and the second harmonic P_{2f}. The generated third harmonic signals (P_{3f}) are measured by the spectrum analyzer. The noise floor of the spectrum analyzer is $-140 \sim -145$ dBm, depending on frequency and averaging time.

Note that the bulk Nb sample is a tensile testing sample that has an etched surface and came from the outer perimeter of the Nb ingot, where thermal strain due to ingot cooling was large. This sample has a high Residual-Resistance Ratio (RRR ~ 200) (with $T_c = 9.2\,K$) and goes through the same material processing steps as a bulk Nb cavity.[26–28] Many single-fixed-point P_{3f} measurements are performed on the essentially undeformed shoulder region inside the marked rectangle (see the schematic diagram of the bulk Nb sample in Fig. 1), where the surface is comparatively flat, permitting close probe/sample separation. An optical reflection image of the bulk Nb surface from the marked region shows a rough surface topography resulting from etching used to remove 20 μm of the surface layer of side F of two strained single crystal tensile samples that were welded together (orientations F and C), as described in Ref. 26.

A good thermal anchoring of the sample is required to ensure that the surface is superconducting, and a thermometer is placed on the bulk Nb top surface to monitor the temperature of the relevant surface. In order to control the height of the probe over the sample, we perform a resonant frequency measurement of the probe assembly as a function of probe/sample separation. The resonant frequency is used as the excitation frequency in the third harmonic response experiment. From our previous nonlinearity measurement and modeling on Nb thin films,[13] the probe height is approximately several hundred nm from the superconductor surface and creates a field parallel to the surface up to the level of the thermodynamic critical field of Nb at 0 K. The details of the probe height control are discussed in Ref. 29.

Figure 2 shows the representative measurements for the power dependence of P_{3f} with respect to the fundamental input power P_f at several fixed temperatures under 5.36 GHz excitation of one fixed location on bulk Nb. The curve measured at T = 20 K indicates the probe third harmonic response P_{3f}^{probe} on the surface of Nb in the normal state. The probe shows third harmonic response only at excitation powers of 15 dBm and above. This is because the magnetic write head is made of ferrite which has hysteretic characteristics and generates background nonlinearity.[12] For measurement below T_c, all curves (at temperature $T_1, T_2 \cdots, T_5$) show a sharp P_{3f} onset from the noise floor of the spectrum analyzer and then follow a continuous increase of nonlinearity until a turnover at high excitation power. After the turnover, the nonlinearity goes down until it approaches the curve of probe nonlinearity P_{3f}^{probe}. After that point, the measured nonlinearity oscillates around the curve of probe nonlinearity.

The onset of the nonlinear response is temperature dependent and can be defined as a temperature dependent lower critical power P_{c1}, a minimum power to excite this nonlinearity above the noise floor. One can clearly see the relation of P_{c1} for each temperature is $P_{c1}^{T_5} > P_{c1}^{T_4} > P_{c1}^{T_3} > P_{c1}^{T_2} > P_{c1}^{T_1}$. That is to say, the onset of nonlinearity requires higher excitation power at lower temperatures. In addition, after the turnover, all $P_{3f}(P_f)$ curves tend to decrease with increasing power, in a power-law manner suggesting that we are suppressing superconductivity locally on the sample. The linear

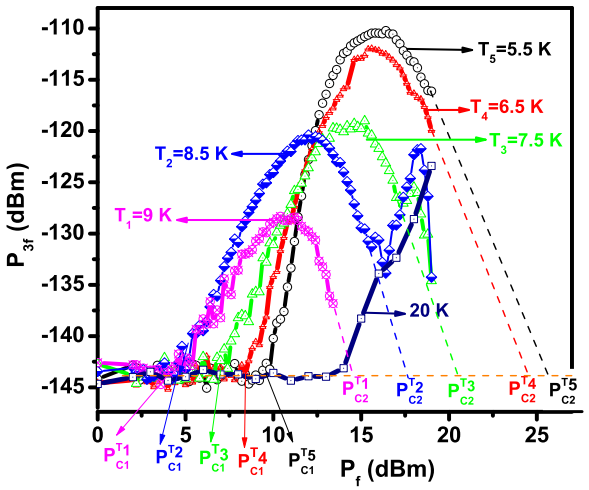

FIG. 2. The P_{3f} dependence on P_f at some specific temperatures for 5.36 GHz local microwave excitation of bulk Nb with the magnetic write head probe. Note the T_c of the bulk Nb sample is 9.2 K. The P_{3f} at $T = 20$ K results from the probe nonlinearity itself. $P_{c1}^{T_5}$ indicates the lower critical power, P_{c1}, at temperature T_5. $P_{c2}^{T_5}$ indicates the upper critical power, P_{c2}, at temperature T_5, and the others have analogous definition. Note that in the measurement, $T_5 = 5.5$ K, $T_4 = 6.5$ K, $T_3 = 7.5$ K, $T_4 = 8.5$ K, $T_1 = 9$ K. The horizontal red line is the spectrum analyzer noise floor.

This article is copyrighted as indicated in the article. Reuse of AIP content is subject to the terms at: http://scitation.aip.org/termsconditions. Downloaded to IP: 129.2.40.52 On: Fri, 19 Sep 2014 14:46:55

extrapolation of P_{3f} to the noise floor can be heuristically defined as an upper critical power P_{c2}, which suggests that superconductivity will eventually be annihilated in high RF magnetic field. Clearly, the relation of P_{c2} for each temperature is $P_{c2}^{T_5} > P_{c2}^{T_4} > P_{c2}^{T_3} > P_{c2}^{T_2} > P_{c2}^{T_1}$. In addition, the slope after each onset is increasing with decreasing temperature. The increase of P_{c1} and P_{c2} with decreasing temperature is consistent with the temperature dependent critical fields of bulk Nb. A summary for both the temperature dependent P_{c1} and P_{c2} are plotted together in the inset of Fig. 3.

An analysis of the temperature dependent P_{c2} at $T_1, T_2, \cdots, T_5$ can be used to estimate the surface field excited by the magnetic write head probe. Generally, the relation between P_{c2} and B_c can be written as $P_{c2}(T) = n[B_c(T)]^2$, where n is a constant relating the incident power in the probe to the RF magnetic field experienced by the Nb surface. The solid curve in Fig. 3 shows the temperature dependent thermodynamic critical field of bulk Nb which is approximated by $B_c(T) \cong B_c(0K)[1 - (\frac{T}{T_c})^2]$ with $B_c(0K) = 0.20\,\mathrm{T}$[3] for the zero temperature thermodynamic critical field of Nb. Note that the value of $B_c(0\,K)$ depends on the quality of Nb, characterized by degree of crystallization, annealing, processing, etc. We assume that our high-RRR Nb sample can achieve the BCS theoretical value at zero temperature. The points in Fig. 3 are the experimental fit of $B_{c2}(T)$ by adjusting the value of n to fit the experimental P_{c2} data. From the field scale generated by a High Frequency Structure Simulator (HFSS) model of the probe[13] and an analytical model of field distribution on the superconductor utilizing the Karlqvist equation,[21] the surface field is on the scale of zero temperature thermodynamic critical field of Nb at a sample/probe separation of several hundred nanometers. When $n = 25.6\,\mathrm{W/T^2}$, the model and the experimental P_{c2} data have minimum deviation. From the fit, the concentrated RF-field on the bulk Nb surface reaches ~120 mT.

The local Ginzburg-Landau parameter (κ) is also estimated assuming $\sqrt{P_{c1}} \propto B_{c1} = \frac{ln\kappa}{\sqrt{2}\kappa} B_c$ and $\sqrt{P_{c2}} \propto B_{c2} = \sqrt{2}\kappa B_c$.[30] The result shows a slowly decreasing κ with increasing temperature (from $\kappa = 0.81$ at $\mathrm{T} = 5.5\,\mathrm{K}$ to $\kappa = 0.72$ at $\mathrm{T} = 9\,\mathrm{K}$), consistent with expectations for $\kappa(T)$[30] and high quality Nb.[6] Finally, the same nonlinear measurement performed at other locations shows the same shape of curve but different values of P_{c1} and P_{c2} with ~5 dBm variation. The variation of P_{c1} and P_{c2} may be due to different localized material properties or to probe height variation for each measurement.

The second experiment involves obtaining raster scan nonlinear response image for a high quality MgB_2 thin film with thickness 200 nm made by hybrid physical-chemical vapor deposition on a sapphire substrate.[31] The surface of this sample is much smoother than that of bulk Nb. Step motors are attached to the three axis translatable arm on the cryostat. The accurate and the repeatable step size in vacuum[32] is several microns, which currently constrains the spatial resolution of our near field scanning probe microwave microscope. The detailed setup of the three axes stepping motor system is discussed in Refs. 29 and 32. The experiment is performed at $\mathrm{T} = 15\,\mathrm{K}$ under 5.33 GHz and 16 dBm microwave excitation. The excitation power is determined from the power dependence measurement as the maximum excitation power before the onset of the probe nonlinearity while in proximity to the MgB_2 sample in the normal state. The power dependent $P_{3f}(P_f)$ and temperature dependent $P_{3f}(T)$ at a fixed position are very similar to that of 50 nm thick films which are discussed in Ref. 21, except the disappearance of intrinsic nonlinearity around $T_c \cong 39\,\mathrm{K}$ due to its greater thickness. The scan is along the x direction, and the probe rasters in y without lifting. The step sizes for both x-axis and y-axis motors are 10 μm in this raster scan. Fig. 4 shows the P_{3f} image on the MgB_2 sample. The P_{3f} contrast shows stronger harmonic signal at the right part of the image, which may result from higher nonlinearity from moving vortices, higher dissipation along grain boundaries near this area, or contrast from weak links between each grain under the strong localized excitation. Another possibility is that MgB_2 intrinsic nonlinearity arising from Josephson coupling between the σ and π bands[33] dominates the nonlinear mechanisms at $\mathrm{T} = 15\,\mathrm{K}$ and overwhelms the dissipation nonlinear mechanisms.

In summary, a clear reproducible nonlinear response signal from the surface of superconducting bulk Nb is obtained by the magnetic write head probe. The nonlinear excitation and localized suppression of superconductivity on high-RRR bulk Nb in the GHz frequency regime indicates the localized

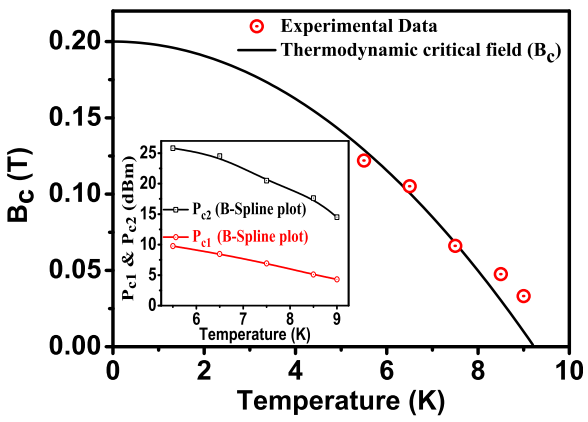

FIG. 3. A fit of the experimental temperature dependent thermodynamic critical field $B_c(T)$ (dot points) with the approximate equation (solid line): $B_c(T) \cong B_c(0K)(1 - (T/T_c)^2)$. The dot points are the calculated B_c from the experimental P_{c2} in Fig. 2. The inset is the temperature dependent P_{c1} and P_{c2} extracted from the data on bulk Nb shown in Fig. 2.

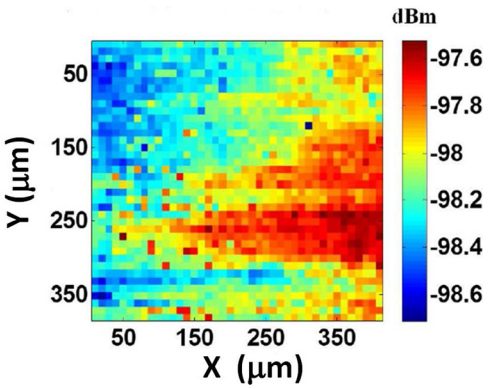

FIG. 4. A P_{3f} image on an MgB_2 thin film with thickness 200 nm. This image is taken at $\mathrm{T} = 15\,\mathrm{K}$ under 5.33 GHz and 16 dBm microwave excitation. Each pixel is 10 μm × 10 μm in size.

This article is copyrighted as indicated in the article. Reuse of AIP content is subject to the terms at: http://scitation.aip.org/termsconditions. Downloaded to IP: 129.2.40.52 On: Fri, 19 Sep 2014 14:46:55

magnetic field from the magnetic write head probe is on the order of the thermodynamic critical field of Nb with $B_{surface} \sim 10^2$ mT. This unique concentrated RF-field has great potential to identify the spatially resolved electrodynamic properties of SRF cavity materials. The raster scan harmonic image of the MgB_2 thin film demonstrates the capability of large area scanning to identify the defects that cause breakdown of SRF cavities.

We thank the referees for helpful suggestions. This work was supported by the US DOE/HEP through Grant No. DESC0004950, and also by the ONR AppEl, Task D10 (Award No. N000140911190), and CNAM. The work at MSU was supported by DOE-OHEP, Contract No. DE-S0004222. The work at Temple University was supported by DOE under Grant No. DE-SC0004410.

[1]G. Ciovati and J. Halbritter, Physica C **441**(1–2), 57–61 (2006).
[2]G. Ciovati, G. Myneni, F. Stevie, P. Maheshwari, and D. Griffis, Phys. Rev. Spec. Top. Accel. Beams **13**, 022002 (2010).
[3]H. Padamsee, J. Knobloch, and T. Hays, *RF Superconductivities for Accelerators*, Wiley Series in Beam Physics and Accelerator Technology (Wiley, 1998).
[4]Z.-H. Sung, P. J. Lee, and D. C. Larbalestier, IEEE Trans. Appl. Supercond. **24**, 68–73 (2014).
[5]J. Halbritter, J. Supercond. **8**(6), 691–703 (1995).
[6]N. Valles and M. Liepe, "The superheating field of niobium: theory and experiment," in *Proceedings of SRF2011*, Chicago, IL USA, (2011), Paper No. TUIOA05, p. 293.
[7]C. P. Vlahacos, J. Matthews, and F. C. Wellstood, IEEE Trans. Appl. Supercond. **21**(3), 412–415 (2011).
[8]N. Kikuchi, S. Okamoto, and O. Kitakami, J. Appl. Phys. **105**, 07D506 (2009).
[9]S. M. Anlage, V. V. Talanov, and A. R. Schwartz, "Principles of near-field microwave microscopy," in *Scanning Probe Microscopy: Electrical and Electromechanical Phenomena at the Nanoscale*, edited by S. V. Kalinin and A. Gruverman (Springer-Verlag, New York, 2006), pp. 207–245.
[10]T. Tai, B. G. Ghamsari, and S. M. Anlage, J. Appl. Phys. **115**, 203908 (2014).
[11]F. H. Liu, S. Shi, J. Wang, Y. Chen, K. Stoev, L. Leal, R. Saha, H. C. Tong, S. Dey, and M. Nojaba, IEEE Trans. Magnetics **37**(2), 613–618 (2001).
[12]T. Tai, X. X. Xi, C. G. Zhuang, D. I. Mircea, and S. M. Anlage, IEEE Trans. Appl. Supercond. **21**, 2615 (2011).
[13]T. Tai, B. G. Ghamsari, and S. M. Anlage, IEEE Trans. Appl. Supercond. **23**, 7100104 (2013).
[14]T. Tajima, A. Canabal, Y. Zhao, A. Romanenko, B. H. Moeckly, C. D. Nantista, S. Tantawi, L. Phillips, Y. Iwashita, and I. E. Campisi, IEEE Trans. Appl. Supercond. **17**, 1330 (2007).
[15]X. X. Xi, Supercond. Sci. Technol. **22**, 043001 (2009).
[16]S.-C. Lee and S. M. Anlage, IEEE Trans. Appl. Supercond. **13**, 3594 (2003).
[17]S.-C. Lee and S. M. Anlage, Appl. Phys. Lett. **82**, 1893 (2003).
[18]S.-C. Lee, M. Sullivan, G. R. Ruchti, S. M. Anlage, B. Palmer, B. Maiorov, and E. Osquiguil, Phys. Rev. B **71**, 014507 (2005).
[19]S.-C. Lee, S.-Y. Lee, and S. M. Anlage, Phys. Rev. B **72**, 024527 (2005).
[20]D. I. Mircea, H. Xu, and S. M. Anlage, Phys. Rev. B **80**, 144505 (2009).
[21]T. Tai, B. G. Ghamsari, T. Tan, C. G. Zhuang, X. X. Xi, and S. M. Anlage, Phys. Rev. Spec. Top. Accel. Beams **15**, 122002 (2012).
[22]D. E. Oates, Y. D. Agassi, and B. H. Moeckly, IEEE Trans. Appl. Supercond. **17**(2), 2871–2874 (2007).
[23]S. Y. Yamamoto and S. Schultz, Appl. Phys. Lett. **69**, 3263 (1996).
[24]S. Y. Yamamoto and S. Schultz, J. Appl. Phys. **81**, 4696 (1997).
[25]C. Jeffries, Q. H. Lam, Y. Kim, L. C. Bourne, and A. Zettl, Phys. Rev. B **37**, 9840 (1988).
[26]D. Baars, H. Jiang, T. R. Bieler, A. Zamiri, F. Pourboghrat, and C. Compton, Applications Of Texture Analysis, A Collection of Papers Presented at the 15th International Conference on Texture in Materials (ICOTOM 15), June 1–6, 2008, Pittsburgh, Pennsylvania, edited by Chief Editor, A. D. Rollett, Ceramic Transactions, Vol. 201 (American Ceramic Society, Westerville, Ohio, 2008), p. 391.
[27]D. Kang, D. C. Baars, T. R. Bieler, and C. C. Compton, AIP Conf. Proc. **1352**, 90–99 (2011).
[28]S. Balachandran, R. C. Elwell, D. Kang, R. E. Barber, T. R. Bieler, and K. T. Hartwig, IEEE Trans. Appl. Supercond. **23**, 7100904 (2013).
[29]T. Tai, Ph.D. dissertation, University of Maryland-College Park, (2013), see http://hdl.handle.net/1903/14668.
[30]M. Tinkham, *Introduction to Superconductivity*, 2nd ed. (McGraw-Hill, New York, 1996), Chap. 5.
[31]X. Zeng, A. V. Pogrebnyakov, A. Kotcharov, J. E. Jones, X. X. Xi, E. M. Lysczek, J. M. Redwing, S. Y. Xu, J. Lettieri, D. G. Schlom, W. Tian, X. Q. Pan, and Z. K. Liu, Nature Mater. **1**, 35 (2002).
[32]R. B. Dinner, M. R. Beasley, and K. A. Moler, Rev. Sci. Instrum. **76**, 103702 (2005).
[33]A. Gurevich and V. M. Vinokur, Phys. Rev. Lett. **90**, 047004 (2003).

This article is copyrighted as indicated in the article. Reuse of AIP content is subject to the terms at: http://scitation.aip.org/termsconditions. Downloaded to IP: 129.2.40.52 On: Fri, 19 Sep 2014 14:46:55